

## **SYNTHESIS AND MAGNETIC PROPERTIES OF COBALT FERRITE MATERIALS**

Min Maung Maung<sup>1</sup>, Thein Tun Linn<sup>2</sup>, and Aung Min<sup>3</sup>

### **Abstract**

Cobalt ferrite powders with general formula  $\text{CoFe}_2\text{O}_4$  was synthesized by sol-gel auto combustion method starting from metal nitrates and citric acid ( $\text{C}_6\text{H}_8\text{O}_7$ ) as a fuel. X-ray diffraction technique (XRD) was used to confirm the crystallite structure and phase formation. The particle size was estimated by the full width half maximum (FWHM) of the strongest X-ray diffraction (XRD) peak (311). The average particle size was observed in the range of 42 to 54 nm. The scanning electron microscopy (SEM) was used to study the grain size, grain distribution of these samples. The dielectric property measurements were carried out by the help of a LCR meter. The dielectric constant and the loss tangent decreases rapidly with increasing frequency, and then reaches a constant value. The room temperature magnetization and demagnetization measurement was done by PERMAGRAPH L apparatus.

**Keywords:** Hysteresis; magnetic properties; remanence; coercivity; Permagraph L; XRD; Grain size.

### **Introduction**

Magnetic materials form an important class of materials used practically in all electric machines such as motors, generators, transformers, relays and electromagnets. With respect to their magnetic behavior, magnetic materials may be classified into diamagnetic, paramagnetic, ferromagnetic, antiferromagnetic and ferrimagnetics. Magnetic ceramics may be divided into one of three different classes; spinel ferrites, hexagonal ferrites and the rare earth ferrites (garnet materials). Ferrites have dc resistivity of many orders of magnitude higher than that of iron and are used for frequencies up to microwave range in transformer cores. They are of greatest interest from the electrical engineering point of view because they have as ferromagnetic materials in as much as they show spontaneous magnetization below a certain temperature [Rajagopal K. (2009)].

Ferrite materials are insulating/semiconductor metal oxides that exhibit moderate saturation magnetization, high coercivity, high electrical resistance, low eddy current and dielectric loss with moderate permittivity. No other material has such a wide range of properties and therefore these materials are exploited for vast applications in various fields like transducers, activators, recording media, permanent magnets, phase shifters, electrode material for Lithium ion batteries, solid oxygen fuel cells and computer technology. In addition with, the ferrite nanoparticles are used in magnetic fluids, humidity and gas sensors, drug delivery etc [Ranjit Kumar Panda, (2015)].

The ferrites exhibit dielectric properties and do not conduct electricity easily therefore ferrites became an alternative for the metal magnets like iron, nickel which conduct electricity readily. Therefore, the processing of these materials is important to modify its properties as per the desired applications. Ferrites are classified into three types depending on the structure namely spinel, garnets and hexagonal ferrites. Garnets have the general formula  $\text{M}_3\text{Fe}_5\text{O}_{12}$  where  $\text{M} = \text{Y}$ ,

---

<sup>1</sup> Dr, Associate Professor, Department of Physics, University of Yangon.

<sup>2</sup> Lecturer, Department of Physics, Hpaan University.

<sup>3</sup> Lecturer, Department of Physics, Mawlamyine University.

Sm, Eu, Gd, Tb etc. and have applications in microwave systems. The hexagonal ferrites represented by the formula  $Me_2Fe_{12}O_{19}$  where  $M = Ba, Sr, Ca$  are important in permanent applications. The spinel ferrites are represented by the general formula  $MFe_2O_4$  where  $M$  is the divalent cation  $M = Co, Mn, Zn, Ni, Cd$  [Ranjit Kumar Panda, (2015)].

Among all the ferrites, cobalt ferrite is one of the potential candidates which exhibit moderate saturation magnetization, high coercivity, electrical insulation with low eddy current loss, and chemical stability etc. Therefore it has been extensively used in high density storage, transformer core, high quality filters, phase shifters etc. Cobalt ferrite is selected as representative for the spinel ferrites to study the electric and magnetic properties and relate its structural modifications. Bulk cobalt ferrite has inverse spinel structure that shifts to partial inversion for nano ferrites [Ranjit Kumar Panda, (2015)].

In this research work, cobalt ferrite was prepared by sol-gel auto combustion method. The structural property, the surface morphology and the bond structural properties were also analyzed by X-ray diffraction (XRD), scanning electron microscope (SEM) and Fourier transforms Infrared (FTIR) spectroscopy. The optical band gap of this material was also investigated by the aid of UV-Vis spectroscopy. The frequency dependence dielectric properties and magnetization behavior were also determined by LCR meter and PERMAGRAPH L technique.

## 2. Experimental procedure

Cobalt nitrate  $Co(NO_3)_2 \cdot 6H_2O$ , ferric nitrate  $Fe(NO_3)_3 \cdot 9H_2O$ , citric acid and liquor ammonia have been used as starting materials for preparation of cobalt ferrites by the sol-gel auto-combustion method. Stoichiometry amounts metal nitrates were dissolved in minimum amount of mixture solution of deionised water and poly ethylene glycol (5:1) separately to make clear solution and citric acid was dissolved in a separate beaker, finally three solutions are mixed in another beaker. The opaque solution was then vigorously stirred for a few minutes in order to have a lucid and homogeneous solution. A small amount of liquor  $NH_3$  was added to the solution to adjust the pH value at 7. The final solution was simultaneously heated and mixed using magnetic stirrer. The solution was heated gradually up to  $100^\circ C$ , to evolve reddish brown color gases and finally the dried gel was burnt-out completely to form loose powders. The obtained powder was sintered at  $900^\circ C$ ,  $1000^\circ C$  and  $1100^\circ C$  for 4 hr. The flow chart of sample preparation was shown in figure 1.

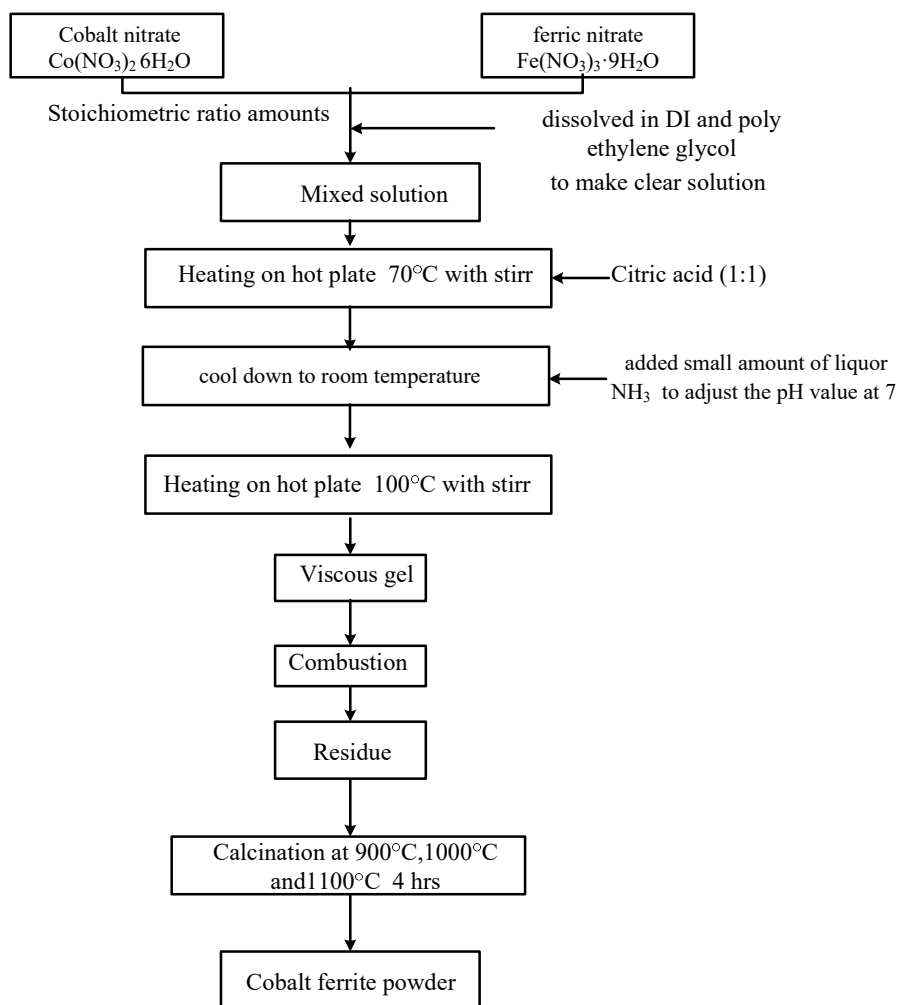


**Figure 1** The flow chart of preparation of cobalt ferrite

## Results and Discussion

### 3.1 XRD analysis

X-rays powder diffraction of the samples was carried out at room temperature using Shimadzu model: XRD 6100 using  $\text{CuK}_\alpha$  ( $\lambda = 0.154 \text{ nm}$ ) radiation, with a diffraction angle between  $20^\circ$  and  $70^\circ$  to check the formation of the required product and structural related properties. The model unit cell of  $\text{CoFe}_2\text{O}_4$  was shown in figure 2. The XRD patterns of the bulk cobalt ferrite nanoparticles annealed at  $900^\circ\text{C}$ ,  $1000^\circ\text{C}$  and  $1100^\circ\text{C}$  were shown in Figure 3(a), (b) and (c). The strongest reflection comes from the [311] plane, which denoted the spinel phase. The peaks indexed to [111], [220], [311], [222], [400],[422], [511] and [440] planes of a cubic unit cell, all planes were the allowed planes which indicated the formation of cubic spinel in single phase and no other impurity phases. The average crystallite size of these samples could be calculated using Scherrer's formula ( $\text{FWHM} = 0.299$  broadening peak (311), angle  $35.5^\circ$ ). The average crystallite size and their porosity were listed in table 1.

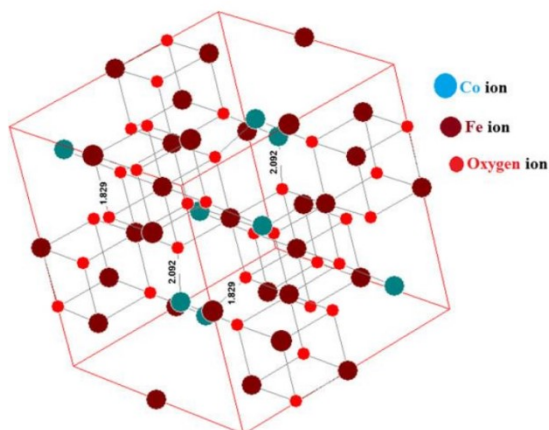


Figure 2 The unit cell of cobalt ferrite[Ranjit Kumar Panda, (2015)].

Table 1 The average crystallite size of cobalt ferrite

Annealing temperature	Lattice parameter $a = b = c$ (Å)	Crystallite size (nm)	X-ray Density ( $\text{g cm}^{-3}$ )	Measured Density ( $\text{g cm}^{-3}$ )	Porosity (P)
900°C	8.36	42.36	5.33	4.05	0.23
1000°C	8.33	45.53	5.33	3.83	0.28
1100°C	8.37	53.05	5.33	3.87	0.27

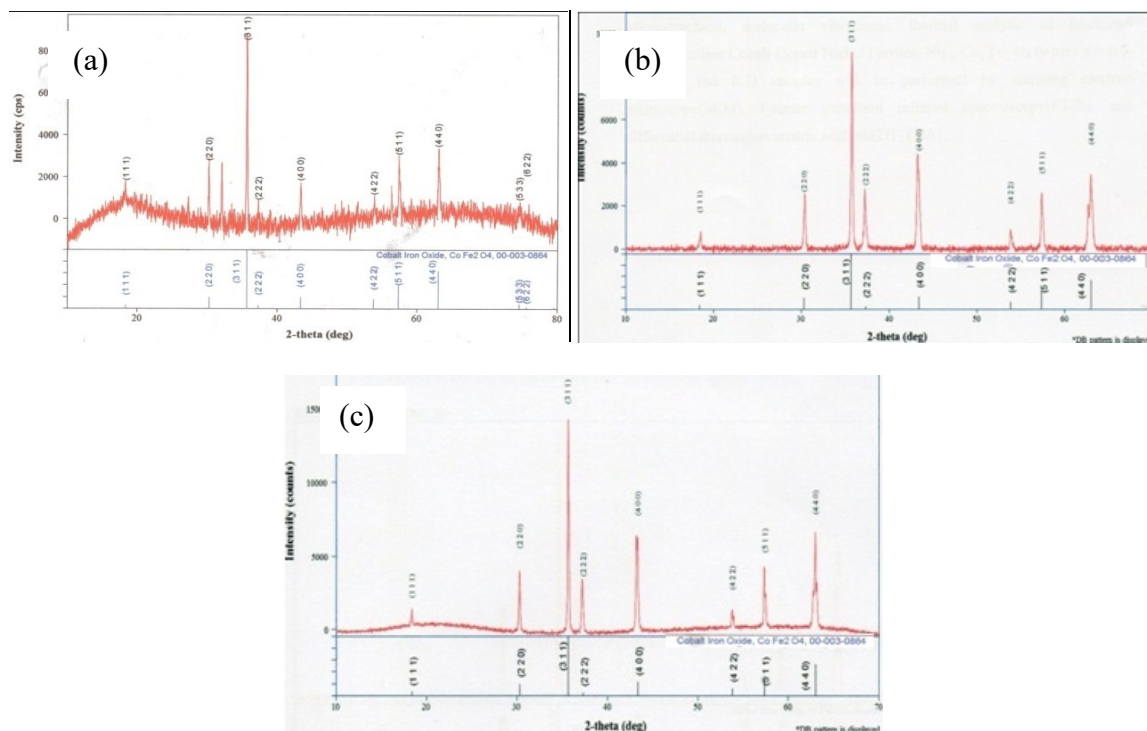
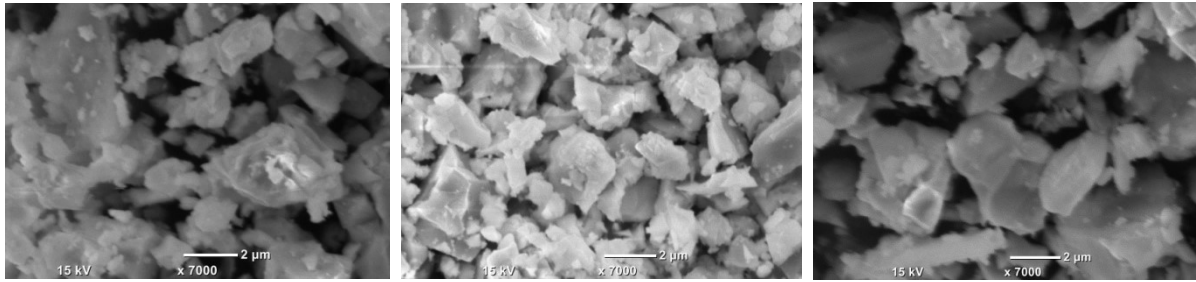


Figure 3 The XRD pattern of cobalt ferrite annealed at (a) 900°C (b) 1000°C (c) 1100°C

### 3.2 SEM analysis

The morphology and the distribution of  $\text{CoFe}_2\text{O}_4$  nanoparticles were determined using SEMJEOL (JSM-67001). Typical SEM images of  $\text{CoFe}_2\text{O}_4$  synthesized particles were shown in Figure 4. SEM micrograph depicted that the samples contain micrometrical aggregation of tiny

particles. The existence of high dense agglomeration indicated that pore free crystallites are present on the surface. Two types of grain growth were observed. The first type was around 10  $\mu\text{m}$  and second type was 2  $\mu\text{m}$ .



**Figure 4** The SEM image of cobalt ferrite annealed at (a) 900°C (b) 1000°C (c) 1100°C

### 3.3 FTIR Analysis

In order to determine the chemical structure of the sample, the FTIR spectrum was observed cobalt ferrite in the frequency range of 4000-800  $\text{cm}^{-1}$  as shown in Figure 5. The decomposition of hydroxide to oxide phase for the formation of spinel ferrites was well reflected in the FTIR spectrum. It had been reported that the IR bands of solids were usually attributed to the vibration of ions in the crystal lattice. The bands around 601  $\text{cm}^{-1}$  and 461  $\text{cm}^{-1}$  represented tetrahedral and octahedral modes of  $\text{CoFe}_2\text{O}_4$ , respectively. The band located around 3336  $\text{cm}^{-1}$  could be attributed to the symmetric vibration of -OH groups. The peak at 1616.4 was related to the O-H vibrations related to the adsorbed water.

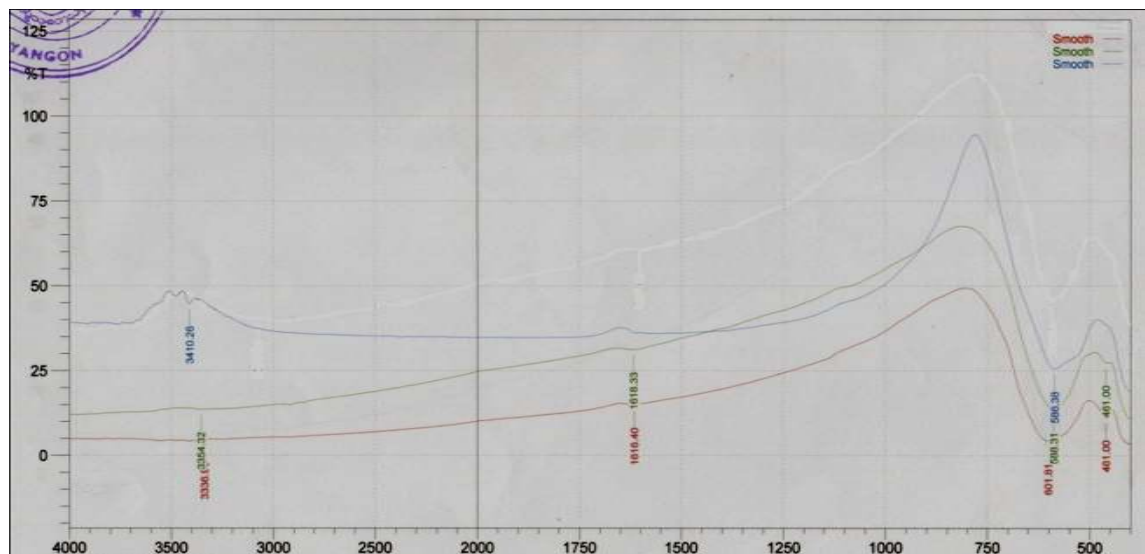


**Figure 5** The FTIR spectrum of cobalt ferrite samples annealed at 900°C, 1000°C and 1100°C

### 3.4 UV-Vis measurement

The plot of  $(\alpha h\nu)^2$  versus photon energy ( $h\nu$ ) was shown in figure 6. In the direct transition, the absorption coefficient ( $\alpha$ ) related with the optical band gap ( $E_g$ ) is given by,  $\alpha h\nu = A(h\nu - E_g)^{1/2}$ , where  $h\nu$  is the photon energy and  $A$  is a constant for a direct transition. The energy gap  $E_g$  could be estimated from the intercept of  $(\alpha h\nu)^2$  vs  $h\nu$  for direct transitions. By extrapolating the linear portion of the energy axis at zero absorption gives the direct band gap of these materials. The energy gap of this sample was observed to be 3.24 eV.

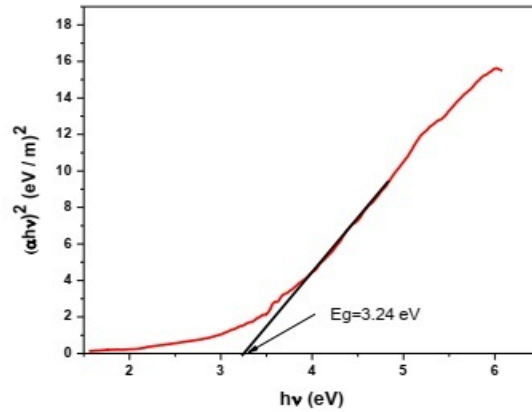


**Figure 6** The estimated energy band gap value of  $\text{CoFe}_2\text{O}_4$  sample ( $1000^\circ\text{C}$ )

### 3.5 Dielectric Properties

The dielectric properties of the ceramic  $\text{CoFe}_2\text{O}_4$  were analyzed using GW Instek 8110 LCR meter over the frequency range 100Hz- 2MHz. The dielectric constant of  $\text{CoFe}_2\text{O}_4$  was studied at different temperatures. For measurements, the samples were obtained with the diameter of  $\sim 13$  mm and thickness  $\sim 2$  mm pellets; it was placed between the silver electrodes having a conventional two terminal sample holder with applied temperature. The capacitance of these samples was measured with temperature range 303 to 353 K with 10 K step and frequency ranging from 100 Hz to 2MHz. The variation of dielectric permittivity with temperature at different frequencies was shown in Figure 7. The low frequency regime observes high permittivity value whereas the high frequency regime observes comparatively low value. The relative permittivity value increased with elevation of temperature. The high dielectric permittivity was found at low frequencies and high temperatures. In present study, the maximum temperature of measurement is only 353K and hence no decrease in dielectric permittivity was observed. The low value of the dielectric constant with increasing frequency could be ascribed to the loose or weak bond of ions at the lower frequency range.

The decrease in dielectric constant with frequency was obvious because of the fact that any effect contributing to polarization was found to show lagging behind the applied field at higher and higher frequencies. By increasing the frequency beyond a certain frequency limit, the electron hopping could not follow the electric field fluctuations causing a decrease in the dielectric constant. Koop argued that the dielectric constant at low frequency comes from the grain boundaries which have a high dielectric constant due high resistivity at the grain boundary region. The dielectric constant at high frequency comes from the grains which have a small value of dielectric constant due to low resistivity. At high temperature, space charges near grain boundaries and electrode contacts were activated and had their displacement along the field direction. This caused space charge polarization which was highly temperature dependent.

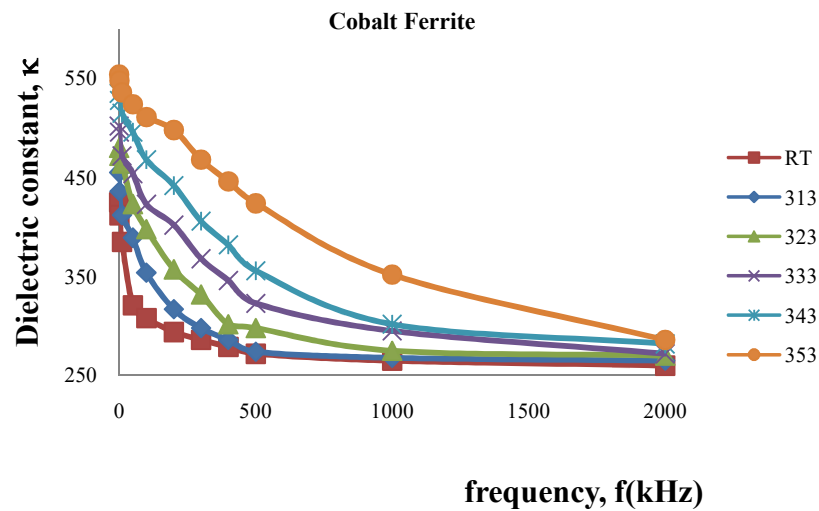


**Figure 7** Dielectric Constant ( $\kappa$ ) behaviour of the  $\text{CoFe}_2\text{O}_4$  samples (1000°C) in the Frequency Range 100Hz to 2MHz

### 3.6 AC Conductivity analysis

Figure 8 represented the ac conductivity behavior of polycrystalline cobalt ferrite. The low temperature region showed a slow transition from a weak frequency dependent conductivity to strong frequency variant part. The fast frequency dependent region appeared at high frequency regime as the conduction process, was due to the localized relaxation hopping mechanism of ions or electrons. According to jumping relaxation model the conductivity in ferrites was due to the hopping mechanism of charge carriers. As frequency approaches relaxation point, charge carriers hop through short distance before the cycle changes. Beyond relaxation frequency, thermal energy could not drive the ions to a long range in order to follow the changing ac cycle rather a localized movement was possible which gave the fast frequency variant region.

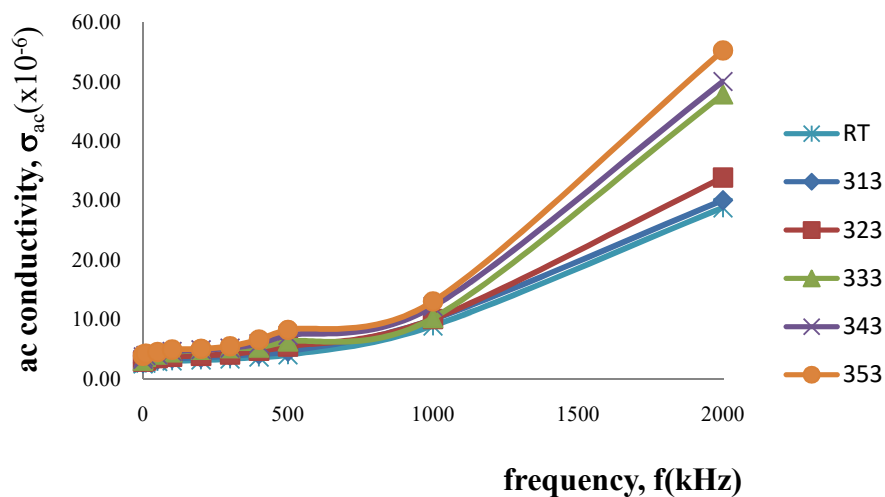


**Figure 8** Variation of AC conductivity of  $\text{CoFe}_2\text{O}_4$  samples (1000°C) with frequency

### 3.7 Magnetic measurements

The magnetic behavior of  $\text{CoFe}_2\text{O}_4$  nanoparticles was investigated using PERMAGRAPH L. Room temperature field dependent magnetic properties of the cobalt ferrite was shown in the figure 9. It exhibited B-H loop at room temperature which represents the ordered state of sample at room temperature. The magnetic property of the cobalt ferrite strongly depends on the cation distribution between the tetrahedral and octahedral sites and grain/particle size of the ferrites. In ferrimagnetic materials net magnetization was equal to difference between the individual magnetic moments of antiferromagnetically interacted octahedral (A) and tetrahedral (B) sites. The estimation of magnetostrictive constant ( $\lambda_s$ ) for the ceramic  $\text{CoFe}_2\text{O}_4$  sample was to be  $13.44 \times 10^{-5}$ . In bulk form cobalt ferrite exhibits inverse spinel structure where cobalt occupies only octahedral site and iron equally distributed in octahedral and tetrahedral sites. The remanent and coercivity value for the  $\text{CoFe}_2\text{O}_4$  nanoparticle was observed about  $8.7338 \times 10^{-3}$  emu/g and 427.03 G respectively.

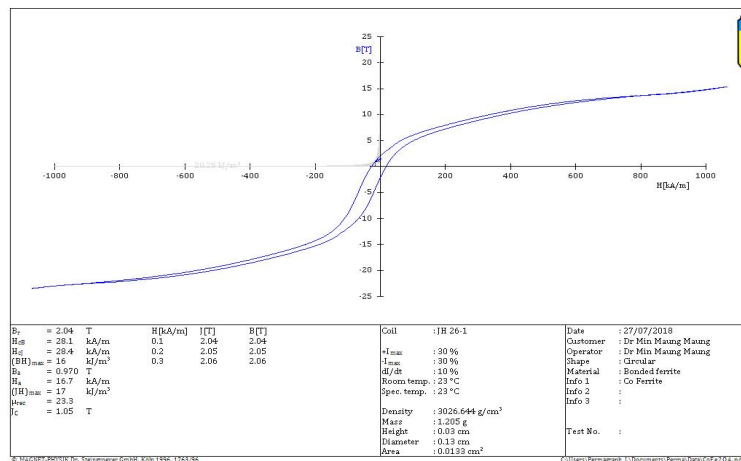


**Figure 9** Room temperature B-H behavior of  $\text{CoFe}_2\text{O}_4$  samples (1000°C)

### Conclusion

The cobalt ferrite ( $\text{CoFe}_2\text{O}_4$ ) samples of different particle size were successfully prepared by nitrate route. The X-Ray diffraction (XRD) patterns of all the samples showed the single phase spinel structure of nanoparticles. FTIR spectrum also supported the formation of  $\text{CoFe}_2\text{O}_4$  attributed to the vibration of ions in the crystal lattice. The surface morphology was observed to be densely packed with irregular grains. From the dielectric studies it became evident that the dielectric constant and the loss decreases rapidly with increasing frequency, and then reaches a constant value. Room temperature B-H loop indicates the orderedness of the ferrimagnetic cobalt ferrite. Low dielectric constants materials were required for high frequency application in electrical circuits, to reduce dielectric losses and skin effect. The high value of electrical resistivity in ferrite was suitable for the high frequency application where eddy current losses are appreciable. The resistivity was decreased with increase in temperature and the material behaved like a semiconductor. Bulk ferrites remained a key group of magnetic materials, while nanostructured ferrites showed a dramatic promise for applications in even significantly wider fields.

## **Acknowledgements**

I would like to express my profound thanks to Professor Dr Khin Khin Win, Head of Department of Physics, and Professor Dr Myo Lwin, Professor Dr Aye Aye Thant, Professor Dr Yin Maung Maung, Department of Physics, University of Yangon, for their kind permission to carry out this work, their encouragement and help during this work.

## **References**

- Moulson A J & Herbert J M (1997) *Electroceramic Materials Properties Applications* (New Delhi: Thomson Press)
- Rajagopal K. (2009) *Textbook of engineering physics part II*. New Delhi-110001.
- Ranjit Kumar Panda, (2015) *Studies on Electric and Magnetic Properties of Cobalt Ferrite and its Modified Systems*, National Institute of Technology, India
- Steingroever GmbH. Dr, (2010), *Computer controlled permagraph® L*” Cologne-Germany.
- Suryanarayana C. and Norton M. G. (1998), *X-ray Diffraction A Practical Approach*, (New York: Plenum)
- Xu Y, (1991) *Ferroelectric Materials and their Applications*, New York: Elsevier Science Publishing Co. Inc.